nature plants

ARTICLES

https://doi.org/10.1038/s41477-019-0566-x

Physiological and evolutionary implications of tetrameric photosystem I in cyanobacteria

Meng Li[1,2,8], Alexandra Calteau[3], Dmitry A. Semchonok[4], Thomas A. Witt[1], Jonathan T. Nguyen[1], Nathalie Sassoon[5], Egbert J. Boekema[4], Julian Whitelegge[6], Muriel Gugger[5] and Barry D. Bruce[1,2,7*]

Photosystem I (PSI) is present as trimeric complexes in most characterized cyanobacteria and as monomers in plants and algae. Recent reports of tetrameric PSI have raised questions regarding its structural basis, physiological role, phylogenetic distribution and evolutionary significance. Here, we examined PSI in 61 cyanobacteria, showing that tetrameric PSI, which correlates with the *psaL* gene and a distinct genomic structure, is widespread among heterocyst-forming cyanobacteria and their close relatives. Physiological studies revealed that expression of tetrameric PSI is favoured under high light, with an increased content of novel PSI-bound carotenoids (myxoxanthophyll, canthaxanthan and echinenone). In sum, this work suggests that tetrameric PSI is an adaptation to high light intensity, and that change in PsaL leads to monomerization of trimeric PSI, supporting the hypothesis of tetrameric PSI being the evolutionary intermediate in the transition from cyanobacterial trimeric PSI to monomeric PSI in plants and algae.

Photosystem I (PSI) is an integral component in the light-dependent reactions of oxygenic photosynthesis in cyanobacteria, algae and plants[1]. Upon illumination, PSI accepts an electron from plastocyanin or cytochrome *c* and transfers this electron to its major acceptor, ferredoxin. Whereas algal and plant PSI have been reported to exist mostly as monomers[2–6], and recently as dimers in spinach thylakoid membrane[7], cyanobacterial PSI has been reported to exist as a trimer in most studies. Trimeric PSI structure has been observed in the cyanobacteria *Synechococcus*[8] and in diverse filamentous and unicellular cyanobacteria[9–17], including the most primitive known cyanobacterium, *Gloeobacter violaceus* PCC 7421[18]. Early protein crystallography structures corroborated these findings of trimeric PSI in cyanobacteria[19,20], such as the structure of trimeric PSI from the thermophilic cyanobacteria *Thermosynechococcus elongatus* BP-1[20]. Because of these early reports, it was assumed that PSI in all cyanobacteria was trimeric, in contrast to the monomeric form found in plants and algae. Recently, a tetrameric form of PSI was observed in the cyanobacteria *Nostoc* sp. PCC 7120[3,21] and *Chroococcidiopsis* sp. TS-821 (TS-821)[22,23], challenging the notion of PSI existing only as a trimer in cyanobacteria. Nevertheless, the PSI tetramer has not been considered as a major oligomeric state in cyanobacteria. Although tetrameric PSI is known to occur in two species, the mechanism controlling the oligomeric assembly and stability remain unknown. Furthermore, the physiological and evolutionary significance of this structural change has yet to be elucidated. A recent cryo-EM structure of PSI tetramer from TS-821 showed that tetrameric PSI is actually a dimer of dimers with two different interaction interfaces between monomers[23]. This structure suggests subtle changes in the placement of the central subunit PsaL, yielding changes in helical bundling that has been implicated as critical in the formation of PSI trimers.

In light of the recent discovery of tetrameric PSI, we investigated a large and diverse set of cyanobacteria to characterize the oligomeric state of PSI structure throughout the cyanobacterial phylum. To investigate an underlying mechanism for tetrameric PSI formation, we probe the correlation between PSI oligomeric states, PsaL sequence and genomic structure using bioinformatics and biochemical techniques. Finally, although the physiological significance of the PSI tetramer is not well understood in cyanobacteria, we have explored several growth conditions that may alter the formation of the tetramer. Our findings indicate that exposure to high light intensity induces a significant increase in PSI tetramer formation, while also increasing carotenoid content. These results shed light on the role and function of higher order oligomers of PSI and provide insight into the possible cyanobacterial lineage associated with the origin of the plastid.

PSI oligomeric states in cyanobacteria

To understand how PSI evolved from its cyanobacterial multimeric forms to the monomeric form in algae and plants, a comprehensive and unbiased understanding of the cyanobacterial PSI oligomeric forms is needed. This requires an investigation of the PSI structures that includes diverse cyanobacteria. Here, we have investigated the oligomeric states of PSI in 61 cyanobacteria including 34 heterocyst-forming cyanobacteria and 5 close unicellular relatives, as well as a set of 22 widely divergent unicellular and filamentous cyanobacteria for comparison (Supplementary Data). For most heterocyst-forming cyanobacteria and their close unicellular relatives (collectively referred to as HCR), blue native polyacrylamide gel electrophoresis (BN-PAGE)

[1]Biochemistry and Cellular and Molecular Biology Department, University of Tennessee, Knoxville, TN, USA. [2]Bredesen Center for Interdisciplinary Research and Graduate Education, University of Tennessee, Knoxville, TN, USA. [3]LABGeM, Génomique Métabolique, Genoscope, Institut François Jacob, CEA, CNRS, Université Evry, Université Paris-Saclay, Evry, France. [4]Electron Microscopy Department, Groningen Biomolecular Sciences and Biotechnology Institute, University of Groningen, Groningen, Netherlands. [5]Collection of Cyanobacteria, Institut Pasteur, Paris, France. [6]Pasarow Mass Spectrometry Laboratory, Geffen School of Medicine, University of California, Los Angeles, CA, USA. [7]Microbiology Department, University of Tennessee, Knoxville, TN, USA. [8]Present address: School of Oceanography, University of Washington, Seattle, WA, USA. *e-mail: bbruce@utk.edu

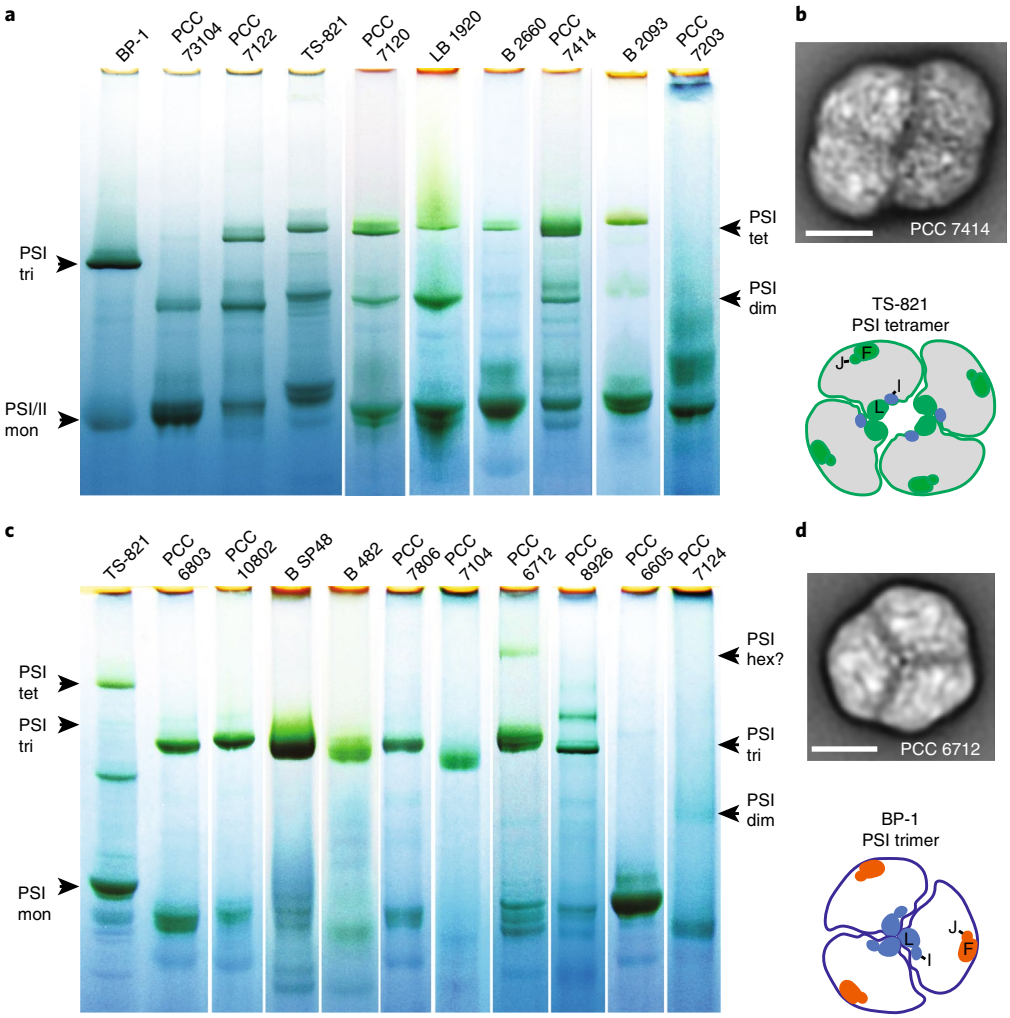

Fig. 1 | Examples of BN-PAGE and TEM analyses of PSI oligomeric states in different cyanobacteria. a, BN-PAGE analyses of the PSI oligomeric states of various heterocyst-forming cyanobacteria and their close relatives. Arrowheads indicate the position of the trimeric form of PSI (PSI tri), the monomeric form of PSI and/or PSII (PSI/II mon), and the dimeric form of PSI (PSI dim). **b**, TEM structure of PSI tetramer from PCC 7414 (top) compared with a TS-821 PSI tetramer model (bottom). **c**, BN-PAGE analyses of the PSI oligomeric states of cyanobacteria that are distantly related to heterocyst-forming cyanobacteria. **d**, TEM structure of PSI trimer from PCC 6712 compared with a BP-1 PSI trimer model. In **a** and **c**, for each strain, the solubilization result of 0.4 mg ml^{-1} Chl in 1% DDM is shown. TS-821, *Synechocystis* sp. PCC 6803 (PCC 6803) and *T. elongatus* (BP-1) are used as controls. The approximate migration distances for photosystem monomer (mon), dimer (dim), trimer (tri), tetramer (tet) and potential hexamer (hex?) are indicated by arrows. All BN-PAGE were performed with at least two technical repeats; BN-PAGE for some strains used for physiology studies was performed more than three times. In **b** and **d**, the locations of PsaL (L), PsaI (I), PsaF (F) and PsaJ (J) subunits are coloured and labelled. Scale bars, 10 nm.

showed the presence of tetrameric and/or dimeric PSI, as well as the abundant monomeric PSI, as the major PSI oligomers (Fig. 1a and Supplementary Fig. 1). Similarly, BN-PAGE analysis of *T. elongatus* BP-1 and *Synechocystis* PCC 6803 consistently indicated the presence of trimeric PSI (Fig. 1a and Supplementary Fig. 1). Specifically, 30 out of 34 heterocyst-forming cyanobacteria, including poorly studied species such as *Spirirestis rafaelensis* UTEX B 2660 (Fig. 1a and Supplementary Fig. 1n), appeared to contain tetrameric or dimeric PSI (Supplementary Data). To verify that the altered electrophoretic mobility was truly indicative of the PSI tetramer, PSI oligomers of several species were examined using transmission electron microscopy (TEM), confirming their tetrameric structure (Fig. 1b and Supplementary Fig. 1). Surprisingly, a few heterocyst-forming cyanobacteria, such as *Anabaena inaequalis* UTEX B381, *Calothrix membranacea* UTEX B379 and *Cylindrospermum licheniforme* UTEX B2014, possessed only monomeric PSI (Supplementary Fig. 1u). *Nostoc* sp. PCC 9335 was the only species of cyanobacteria in the study that had significant amounts of both trimeric and dimeric forms of PSI (Supplementary Fig. 2a). Analysis of the unicellular cyanobacteria that are closely related to the heterocyst-forming cyanobacteria, including TS-821, *Synechocystis* sp. PCC 7509 and *Gloeocapsa* sp. PCC 7428 (Supplementary Fig. 1a,b), showed that they contain more tetrameric, dimeric and monomeric PSI than trimeric PSI. The other two species of *Chroococcidiopsis* that we tested, *Chroococcidiopsis thermalis* PCC 7203 (Fig. 1a and Supplementary Fig. 1c) and *Chroococcidiopsis* sp. PCC 7434 (Supplementary Fig. 2a), contained primarily monomeric PSI with some dimeric PSI. Collectively, these results revealed that besides monomeric PSI, tetrameric and dimeric PSI rather than trimeric PSI comprise the majority of PSI oligomers in the HCR. Trimeric PSI was either not detectable or only present as a minor species in cyanobacteria placed in this clade (Supplementary Data), suggesting that there is a structural and potentially physiological basis for the tendency to form dimeric or tetrameric PSI in these related cyanobacteria.

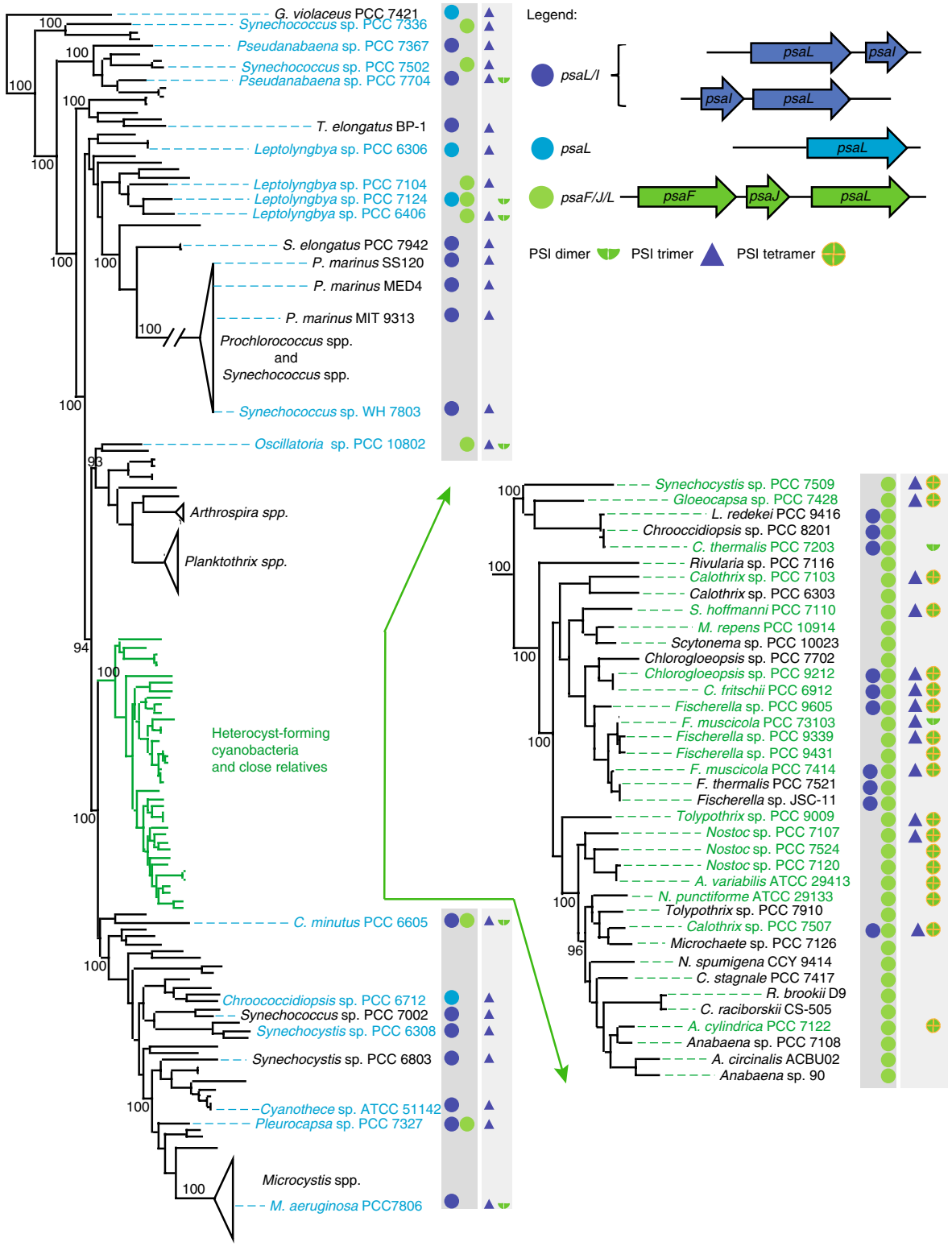

Fig. 2 | Distribution of PSI oligomers and the location of *psaL* genes among cyanobacteria with sequenced genomes. The relative locations of *psaL to psaI, psaF and psaJ* genes are colour coded after each strain number, followed by the observed or reported oligomeric states of PSI in that cyanobacterium. The clade including HCR is expanded for clarity, indicated by green arrows. Strains whose PSI oligomeric states are investigated in this study are coloured in cyan or green. Bootstrap values (%) of some major branches are labelled. A fully expanded species tree is shown in Supplementary Fig. 3.

In contrast to HCR, most other cyanobacteria that we studied contained predominantly trimeric PSI (Fig. 1c, Supplementary Figs. 1 and 2 and Supplementary Data). This trimeric form of PSI can be confirmed by TEM, as shown for PCC 6712 (Fig. 1d). Among this group of PSI trimer-containing cyanobacteria were *T. elongatus* and *Synechocystis* PCC 6803, in which the presence of trimeric PSI has been confirmed by crystallography[23,24]. Many of the other cyanobacteria studied were also observed to

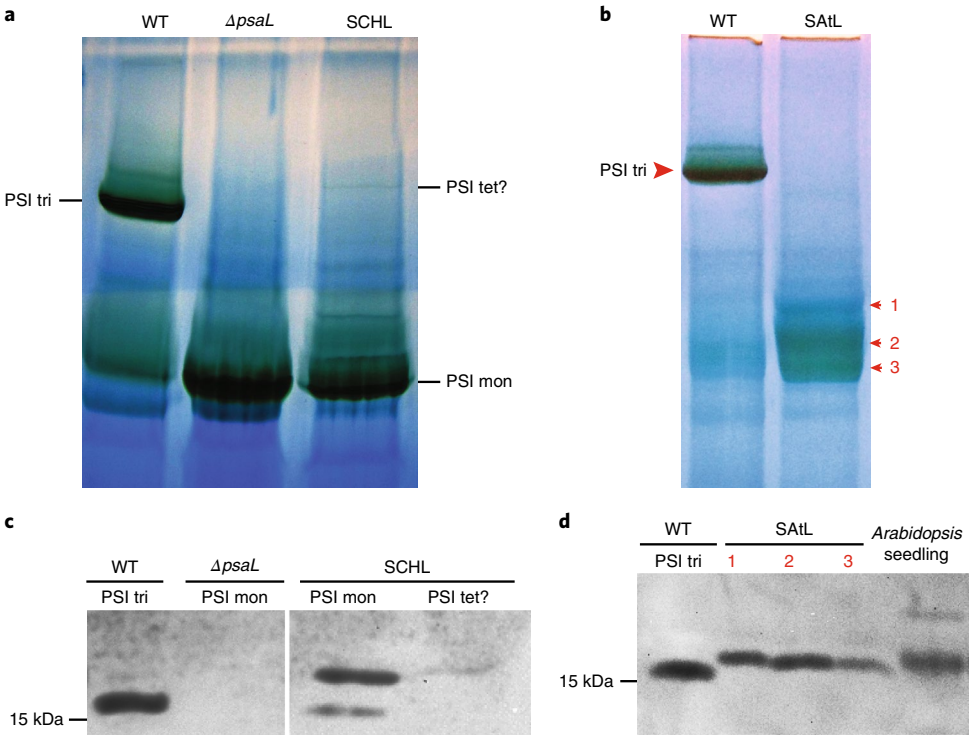

Fig. 3 | BN-PAGE and western blot analyses of PSI oligomers in *Synechocystis* sp. PCC 6803 expressing different PsaL. a, BN-PAGE of solubilized thylakoid membranes from *Synechocystis sp.* PCC 6803 WT, *ΔpsaL* and expressing TS-821 PsaL (SCHL). Slices containing PSI samples were taken from the gel for subsequent SDS–PAGE and western blotting to detect PsaL. Each lane was loaded with solubilized membrane containing 16 μg Chl. **b**, BN-PAGE of solubilized thylakoid membranes from *Synechocystis sp.* PCC 6803 WT and mutant expressing *Arabidopsis thaliana* PsaL (SAtL). **c**, Western blot of the PSI samples from the BN-PAGE analysis in **a**. PSI trimer (tri) from WT, PSI monomers (mon) from *ΔpsaL* and SCHL, as well as potential PSI tetramer (tet?) were analysed. **d**, Western blot of the PSI bands isolated after the BN-PAGE in **b**. Whole *A. thaliana* seedling was used as a control. BN-PAGE of transgenic lines, SCHL and SAtL were done with three independent lines and showed similar monomeric PSI phenotypes. Western blots confirming the presence of exogenous PsaL were performed as two technical repeats.

contain trimeric PSI (Fig. 1c, Supplementary Figs. 1 and 2 and Supplementary Data).

Occasionally, BN-PAGE indicated more unusual PSI oligomers in these diverse cyanobacteria. For example, a potential PSI hexamer was observed in *Chroococcidiopsis* sp. PCC 6712, in equilibrium with the primary PSI trimer in vitro (Fig. 1c,d and Supplementary Fig. 1c,d). Although the BN-PAGE reveals some other minor PSI oligomeric forms in these strains, such as the PSI dimer in *Microcystis* sp. PCC 7806 (Fig. 1c and Supplementary Fig. 2a,b and Supplementary Data), and a potential PSI tetramer in *Planktothrix paucivesiculata* PCC 8926 (Supplementary Fig. 2c), the predominant PSI oligomer in these diverse cyanobacteria is trimeric. In contrast to other PSI trimer-containing strains, the PSI monomer was clearly dominant in *Chamaesiphon minutus* PCC 6605 and *Leptolyngbya* sp. PCC 7124, which harboured substantial amounts of PSI dimers and monomers (Fig. 1c and Supplementary Fig. 2a).

Correlation of PsaL and PSI oligomers

Previous structural studies on cyanobacterial PSI have identified different PsaL–PsaL interactions within the trimeric and tetrameric PSI oligomers[20,23], shown schematically in Figs. 1b,d. Previous work has identified not only subtle differences in the protein sequence of the PsaL subunits, but also a change in the genomic organization and genomic location of *psaL* in the TS-821 cyanobacterial genome[19]. In the context of the larger group of cyanobacteria presented here, we investigated whether this correlation holds true across the different PSI oligomeric forms identified. To allow visualization of the distribution of PSI oligomers within cyanobacteria, we localized the distribution of *psaL* in relation to *psaI*, *psaF* and *psaJ* genes on a species tree (Fig. 2 and Supplementary Fig. 3a). We analysed the *psaL* distribution of cyanobacteria within a known genomic dataset and 14 additional heterocyst-forming strains. In all HCR, the *psaL* gene is located downstream of *psaF* and *psaJ* (*psaF–psaJ–psaL*) (Fig. 2 and Supplementary Fig. 3b), in agreement with an earlier report[22]. This PsaL encoded by *psaF-psaJ–psaL*, along with the prevailing tetrameric and dimeric PSI, clearly delineates the clade of cyanobacteria, namely HCR, represented by the green lines and the inset in Fig. 2.

In cyanobacteria that fall outside of the HCR clade, *psaL* is frequently flanked by *psaI* (*psaL–psaI*) or, in a few cases, it is found as *psaF–psaJ–psaL* or isolated from other *psa* genes altogether (Fig. 2 and Supplementary Fig. 3a). Besides the 9 strains with reported PSI trimers, BN-PAGE analyses of the PSI oligomers identified an additional 16 strains with trimeric PSI (shown in blue text, Fig. 2). These PSI trimer-bearing cyanobacteria, spreading out in the cyanobacteria phylum outside HCR, cover each major branching point and clade. This group also includes the well characterized reference strains *T. elongatus* and *Synechocystis* PCC 6803. Although the absence of PsaL, encoded by *psaF–psaJ–psaL*, is clearly correlated to the presence of PSI trimer in cyanobacteria (Fig. 2), the presence of PsaL does not always indicate a tetrameric or dimeric PSI. The phylogenetic analysis of PsaL revealed that PsaL encoded by *psaF–psaJ–psaL* falls into different lineages, with those in HCR being a distinct clade (dark green in Supplementary Fig. 3b).

Some cyanobacteria with tetrameric PSI, such as *Fischerella muscicola* PCC 7414, also harbour two copies of the *psaL* gene, one copy organized as *psaF–psaJ–psaL* and the second organized

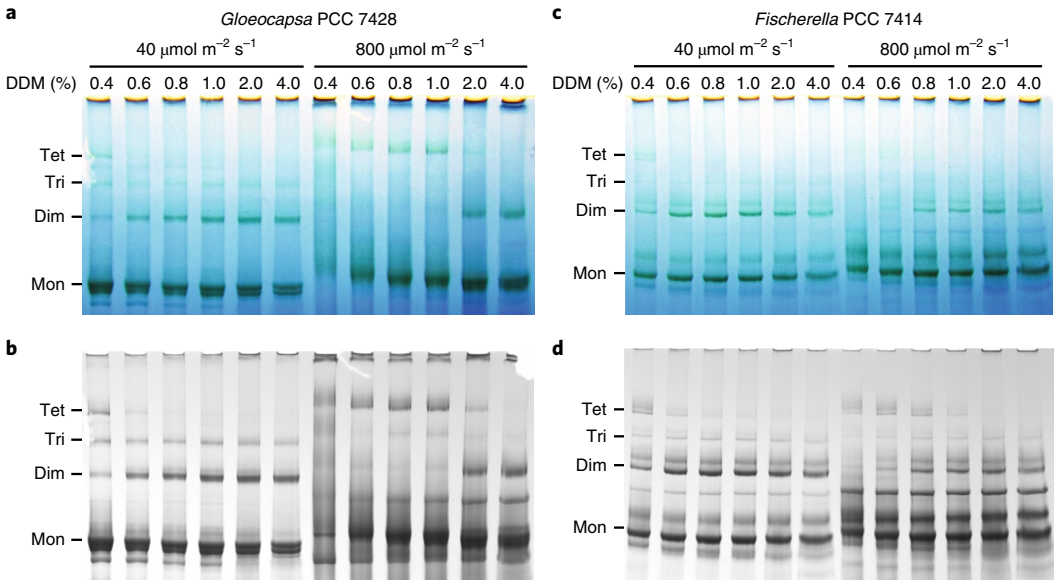

Fig. 4 | BN-PAGE analyses of cyanobacterial PSI oligomeric states under different light intensities. a–d, BN-PAGE of solubilized thylakoid membranes from PCC 7428 (**a**, unstained gel; **b**, Coomassie-stained gel) and PCC 7414 (**c**, unstained gel; **d**, Coomassie-stained gel). Left lanes, LL (40 μmol m^{-2} s^{-1}); right lanes, HL (800 μmol m^2 s^{-1}). Thylakoid membranes with 0.2 mg ml^{-1} Chl were solubilized in different concentrations of DDM (w/v, %) as indicated for each lane. Approximately 1.6 μg Chl was loaded for each condition. Main bands corresponding to PSI monomer (Mon), dimer (Dim), trimer (Tri) and tetramer (Tet) are labelled. BN-PAGE was performed as two technical repeats, which showed similar PSI oligomeric shifts under different light intensities.

as *psaL–psaI* (Fig. 2 and Supplementary Fig. 3a). The copy in *psaF–psaJ–psaL* resembles HCR and indicates tetrameric or dimeric PSI (Supplementary Fig. 3b, coloured in dark green), while the second form of PsaL (in the *psaL–psaI* locus) is closely related to the recently identified far-red-light-responsive PsaL found in monomeric PSI in *Leptolyngbya* sp. strain JSC-1[25] (Supplementary Fig. 3b, coloured in red)[25]. This indicates that some of the HCR may express this *psaL* gene (in *psaL–psaI*) during far-red-light acclimation.

To verify a direct correlation between a specific PsaL protein and the formation of the PSI tetramer, we performed subunit analyses of the isolated PSI trimer and tetramer from three different cyanobacteria, TS-821, PCC 7428 and PCC 7414, using liquid chromatography with tandem mass spectrometry (LC–MS/MS). Of note, for all three species, the same PsaL protein, encoded by *psaL* in *psaF–psaJ–psaL*, was observed in both tetrameric and trimeric PSI (Supplementary Fig. 4). Moreover, genome sequencing of TS-821 revealed only a single form of *psaL*. Although PCC 7414 encodes two copies of the *psaL* gene (Fig. 2), only the PsaL encoded by *psaL* in the *psaF–psaJ–psaL* structure was found in either PSI form isolated under our experimental conditions. These results reinforced the possibility that the *psaL* encoded in *psaL–psaI* in PCC 7414 is an example of a far-red-light-responsive PSI gene[25,26]. These far-red-light-responsive genes have a distinct genomic organization. Moreover, in a maximum-likelihood tree of PsaL, the group of far-red-light-responsive forms of PsaL form a distinct clade (red text, Supplementary Fig. 3b). Phylogenetic analysis revealed that *psaL* from *psaF–psaJ–psaL* loci of HCR form a single clade. However, the observation that the same PsaL is observed in both tetrameric and trimeric PSI in TS-821, PCC 7428 and PCC 7414 suggests that the unique PsaL encoded in *psaF–psaJ–psaL* is necessary, but not sufficient, to direct PSI tetramer formation.

PsaL replacement affects PSI oligomerization

To investigate precisely which structural property of PsaL is key to the determination of the PSI oligomeric state, we performed gene-replacement experiments in the mesophilic cyanobacteria *Synechocystis* sp. PCC 6803. Replacing wild-type (WT) PsaL in *Synechocystis* sp. PCC 6803 by homologous recombination with either TS-821 PsaL or *Arabidopsis* PsaL resulted in monomeric PSI in both mutants (Fig. 3a,b). Western blotting of these monomeric forms of PSI showed that they too contained PsaL bound to PSI (Fig. 3c,d). This observation suggests that the monomerization of PSI in these transgenic lines is not due to the lack of PsaL expression and/or assembly. These findings suggest that small differences in the PsaL structure alone can lead to the monomerization of trimeric PSI in cyanobacteria, as found with the predominantly monomeric PSI in PCC 6605 (Fig. 1c and Supplementary Fig. 2a).

Previous work on TS-821 suggested that the loop in PsaL between the second and third transmembrane helices might have key roles in PSI oligomerization and PsaL evolution[19]. The structure of this loop was not resolved in the trimeric PSI crystal structure from *T. elongatus* (Protein Data Bank ID 1JB0), but subsequent improved plant PSI monomer structures showed the interaction between this loop sequence and PsaH[27,28]. TS-821 PsaL has an unusual multiproline motif in this loop sequence; we therefore examined the conservation of this loop sequence between PsaL second and third transmembrane helices in all HCR in our study in relation to their PSI oligomeric states (Supplementary Fig. 5). Using a logo plot to analyse these regions of all 38 HCR PsaLs, we identified a conserved proline-rich motif, frequently occurring as NPPXP followed by PNPP (Supplementary Fig. 5). Most of the PsaLs from species outside the HCR clade with trimeric PSI lack this motif. However, this motif is shared by both copies of PsaL in PCC 6605 (Supplementary Fig. 5) which has predominantly monomeric PSI (Fig. 1c and Supplementary Fig. 2a). These observations suggest a similar mechanism of trimeric PSI destabilization in PCC 6605, involving a multiproline motif similar to the one in this region of PsaL in the heterocyst-forming cyanobacteria.

Influence of environmental factors

The formation of PSI tetramers is restricted to a specific subset of cyanobacteria; however, although we were able to 'map' this trait to the HCR, there was no clear understanding of the physiological or evolutionary role driving this change in

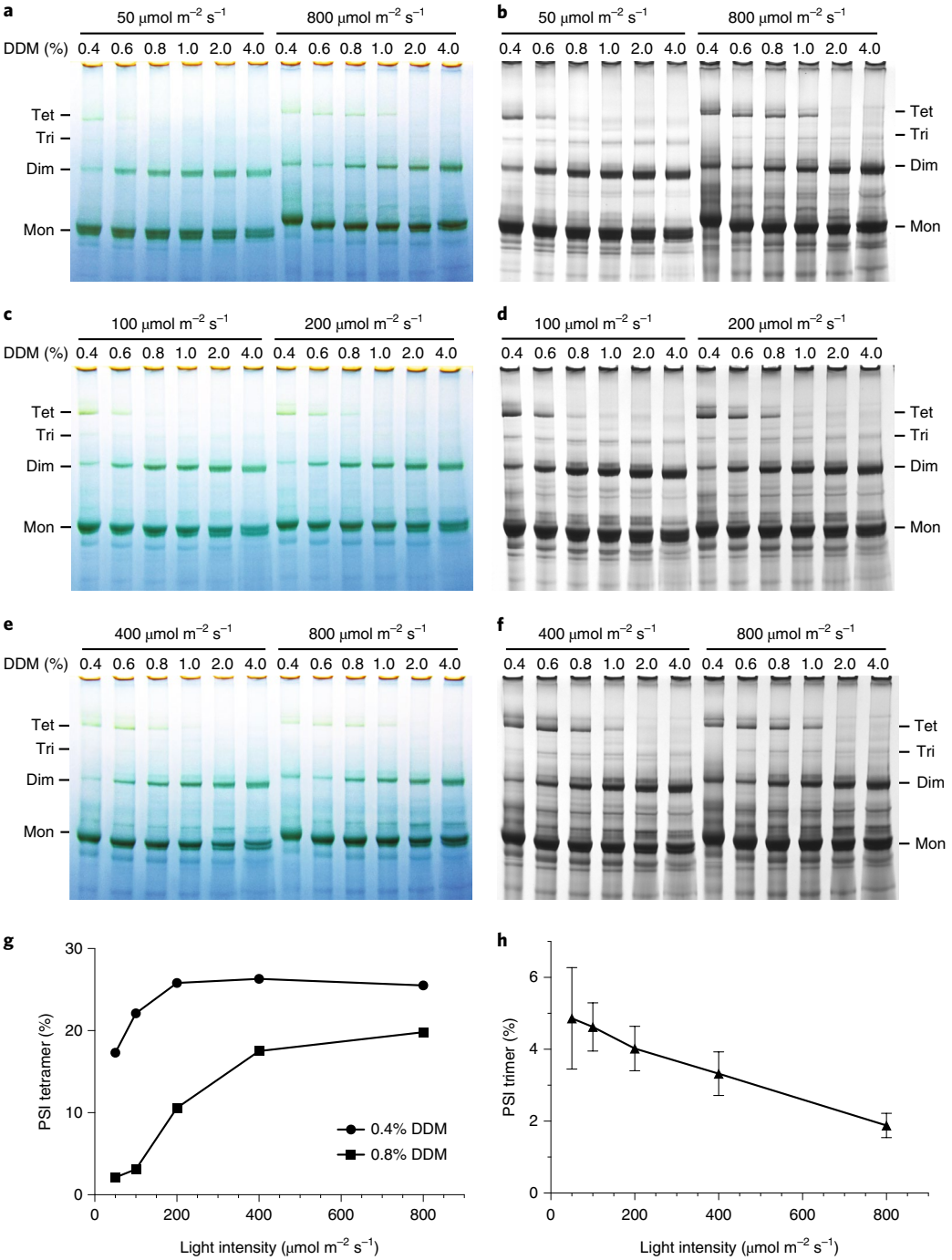

Fig. 5 | Comparison of TS-821 PSI oligomeric profiles under different light intensities. a–f, BN-PAGE of solubilized thylakoid membrane from TS-821 cultured under different light intensities. **a**,**c**,**e**, Unstained gels. **b**,**d**,**f**, Coomassie-stained gels for quantification. Thylakoid membranes with 0.2 mg ml^{-1} Chl were solubilized in different concentrations of DDM (w/v, %) as indicated for each lane. Approximately 1.6 μg Chl was loaded for each condition. Main bands corresponding to PSI monomer (Mon), dimer (Dim), trimer (Tri), and tetramer (Tet) are labelled. **g**, Relative quantities of PSI tetramer under different light intensities. Two solubilization conditions, 0.4% and 0.8% DDM, are presented to show the observed maximum quantities and the stabilities of PSI tetramer under different light intensities. **h**, Relative quantities of PSI trimer under different light intensities. Data are mean ± s.d. ($n = 5$ solubilization conditions for each light intensity, 0.6 to 4.0% DDM). The experiments with incremental light intensities were performed once; the comparisons between HL and LL were performed more than three times.

oligomerization. Since most heterocyst-forming cyanobacteria have tetrameric PSI, the we investigated the influence of nitrogen sources and presence of heterocysts on PSI tetramer formation. We grew three heterocyst-forming strains (PCCC 7414, PCC 7120 and PCC 7122) in both nitrate depleted BG-11 media (BG-110) and BG-11 supplemented with NH_4^+. On the basis of the similar PSI pattern observed with BN-PAGE (Supplementary Fig. 6a) as observed in the strains cultured in standard BG-11 media (Supplementary Fig. 1j,k), the results indicate that the nitrogen sources did not affect the presence of tetrameric PSI.

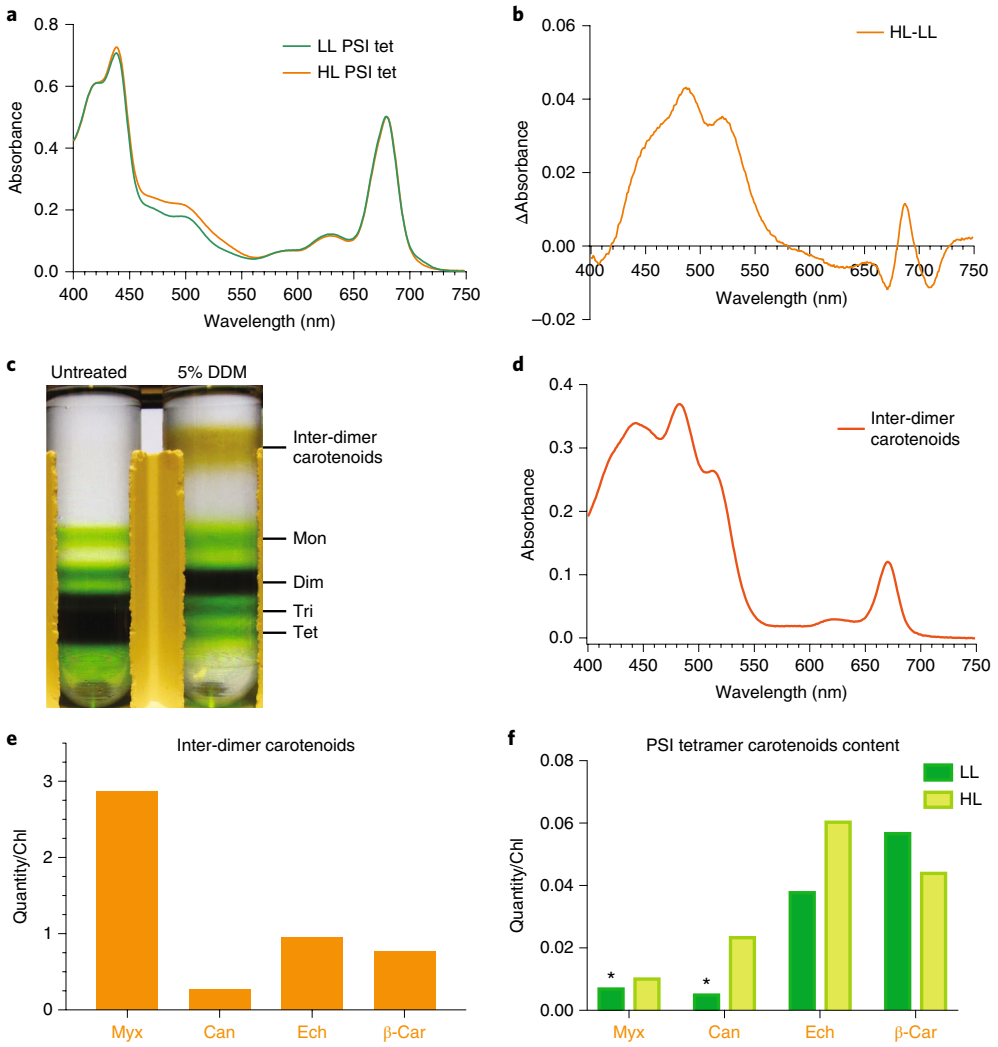

Fig. 6 | The impact of light intensities on tetrameric PSI in TS-821. a, Absorption spectra of PSI tetramers isolated from TS-821 grown under LL and HL conditions. **b**, Difference between HL and LL absorption spectra for PSI tetramers calculated from spectra in **a**. **c**, Sucrose density gradient ultracentrifugation of isolated PSI tetramer. The sample treated with 5% DDM is compared with untreated PSI tetramer. Main bands corresponding to interdimer carotenoids, PSI monomer (Mon), dimer (Dim), trimer (Tri) and tetramer (Tet) are labelled. The release of carotenoids on 5% DDM treatment was observed in all three independent experiments tested. **d**, Absorption spectrum of interdimer carotenoids isolated from treated PSI tetramer after sucrose density gradient ultracentrifugation in **c**. **e**, Quantitative analysis of interdimer carotenoids. **f**, Quantitative comparison of carotenoids in PSI tetramer isolated under HL and LL conditions, presented as the ratio of carotenoids to Chl. The detected carotenoids include myxoxanthophyll (Myx), canthaxanthin (Can), echinenone (Ech) and β-carotene (β-Car). Asterisks denote where detected quantities are below the limit of quantification. Absorption data are the mean of three technical repeats. Pigment analysis data reflect results of one experiment.

Similar results were obtained for *Fischerella* sp. UTEX LB 1829 (BG-110 vs BG-11, Supplementary Fig. 1e). These strains did not develop heterocysts with supplemented NH_4^+, indicating the presence of tetrameric PSI in vegetative cells. The presence of tetrameric PSI in unicellular strains such as TS-821, PCC 7509 and PCC 7428 (Fig. 1a and Supplementary Fig. 1a,b) also agrees with a PSI tetramer independent from heterocyst development, even though tetrameric PSI was shown in heterocysts[29]. In the case of *Nodularia* PCC 73104, the small amount of PSI tetramer was only observed in BG-11 medium (Supplementary Fig. 1j), whereas the addition of NH_4^+ or salt in the culture media appeared to diminish the tetrameric PSI (Supplementary Fig. 6c). The special case of *Nodularia* PCC 73104 needs more studies to elucidate the significance of its response, since *Nodularia* are usually found in brackish or oceanic environments and some strains do not abolish their heterocysts in the presence of NH_4^+ (refs. [30,31]).

Growth temperature had little, if any, effect on the presence of tetrameric or trimeric PSI (Supplementary Fig. 6b) on the four different cyanobacteria investigated. With respect to salinity, we cultured two strains of *Nodularia*—heterocyst-forming cyanobacteria isolated from brackish or saline water—in both fresh water and artificial seawater nutrient medium III (ASNIII); we observed little difference in the amount of the tetramer/dimer (Supplementary Fig. 6c). Salinity also had no effect on the presence and amount of trimeric PSI in *Pseudanabaena* sp. B SP48 (Supplementary Fig. 2e). Together these results suggest that none of the factors presented thus far, i.e. nitrogen source, heterocyst development, temperature stress or salinity, have an effect on the formation of tetrameric and trimeric PSI.

PSI tetramer in response to light intensity

In contrast to the other environmental factors we investigated, altering the light intensity during growth had a clear effect on the ratio

of the PSI oligomeric forms. Our study on TS-821 showed that in response to a change from low light (LL) to high light (HL) intensity, there was accumulation of tetrameric PSI and a decrease in trimeric PSI[23]. To confirm that light intensity was a common factor determining PSI tetramer/trimer ratio, we investigated the HL response of other cyanobacterial strains. We observed an increase in quantity and stability of the tetrameric PSI for both PCC 7428 and PCC 7414 under HL conditions (Fig. 4). In addition, the amount of trimeric PSI was much higher for PCC 7428 when grown at low light (LL) levels (Fig. 4a,b). The difference observed in PCC 7414 under HL versus LL was slightly smaller than that observed in PCC 7428 (Fig. 4c,d) possibly due to self-shading within the intertwined filaments of PCC 7414 (Supplementary Fig. 7). Nevertheless, these results point towards a common HL response, in which tetrameric PSI accumulates and trimeric PSI is suppressed in strains having both forms of the PSI oligomers. Therefore, it is reasonable to speculate that tetrameric PSI is better adapted to HL than trimeric PSI.

We next performed a more detailed study of PSI oligomer profiles for TS-821 cultured under several different light intensities, which supported the hypothesis that tetrameric PSI is an adaption to HL. As shown in Fig. 5, the stability and relative quantity of the PSI tetramer in TS-821 increased as the intensity of light was increased from 50 to 800 μmol m^{-2} s^{-1} (Fig. 5a–g). Plotting the relative amount of PSI tetramer (percentage over all PSI oligomers) against light intensity showed that the apparent maximum increased with light intensity (0.4% *n*-dodecyl-β-d-maltopyranoside (DDM); Fig. 5g). The stability of PSI tetramer, indicated by the relative quantity at higher detergent concentration (0.8% DDM; Fig. 5g), was also enhanced by higher light intensities. By contrast, the relative amount of trimeric PSI decreased almost linearly as the light intensity increased (Fig. 5h). This ability to alter the oligomeric form of PSI is not found in all species of *Chroococcidiopsis*, as indicated by the observation that the absence of PSI tetramer in PCC 7203 was not affected by light intensity (Supplementary Fig. 6d).

To investigate whether tetrameric PSI in TS-821 undergoes a shift in pigment composition, or biochemical or biophysical changes under different light intensities, we compared absorption spectra and 77K fluorescence spectra of different PSI oligomers isolated from cells grown under different light conditions (Fig. 6a,b and Supplementary Fig. 8). Whereas the 77K emission spectra of these isolated PSI oligomers did not show significant differences (Supplementary Fig. 8), tetrameric PSI produced under HL exhibited additional absorption in the range around 440–560 nm compared with tetrameric PSI produced under LL (Fig. 6a,b). The difference spectrum between these two samples showed at least three discernable absorption peaks (450, 490 and 520 nm) (Fig. 6b). The absorption spectrum of the LL PSI tetramer also had a similar additional absorption around 400–500 nm when compared with the PSI trimer under LL (Supplementary Fig. 8).

Interestingly, when the PSI tetramer was treated with 5% DDM and dissociated into dimers, a substantial amount of carotenoids stayed in the top layer of the sucrose gradient after separation by centrifugation (Fig. 6c). It is very likely that these carotenoids are associated with the interdimer interface and may even reside in the centre of the tetrameric structure, only being released upon dissociation. Interestingly, the absorption spectrum of released carotenoids (Fig. 6d) resembled the increased absorbance observed in the HL tetramer (Fig. 6b). Moreover, spectral analysis of the tetrameric PSI in both TS-821 and PCC 7414 reveal an increase in absorption in the range of 400–550 nm compared with the PSI dimer and trimer (Supplementary Fig. 9c,d), resembling the absorption spectrum of the interdimer carotenoids (Fig. 6d). These results suggest that tetrameric forms of PSI are generally rich in carotenoids compared to trimeric and dimeric forms of PSI. When these interdimer carotenoids were isolated and analysed by high-performance liquid chromatography, we identified novel PSI cofactors: myxoxanthophyll, canthaxanthin and echinenone, in addition to the known cofactors chlorophyll (Chl) and β-carotene (Fig. 6e). The semi-quantitative comparison of the HL PSI tetramer and LL PSI tetramer also revealed that tetrameric PSI harboured more myxoxanthophyll, canthaxanthin and echinenone, and less β-carotene (per Chl) under HL (Fig. 6f).

Discussion

Our results indicate that tetrameric PSI is a characteristic shared by most, if not all, heterocyst-forming cyanobacteria and their closest unicellular relatives. The distribution of tetrameric PSI in this clade of cyanobacteria indicates a shared physiological characteristic between the two morphologically distinct cyanobacteria. The previous classification of PCC 7428 and TS-821 would place these cyanobacteria in section II on the basis of their reproduction by multiple fission giving rise to baeocytes[32], but our current work on these PSI dimer and tetramer containing unicellular cyanobacteria support a different placement. Phylogenetic analyses based on the 16S rRNA gene as well as a more universal set of conserved genes suggest that these tetramer-forming cyanobacteria are closely related to heterocyst-forming cyanobacteria[33,34]. However, no further physiological or biochemical evidence had been reported to support the close evolutionary linkage between the two groups. In this study, we have shown similar physiological and biochemical properties of the PSI oligomers observed in those two groups, providing further support of a phylogenetic placement of the unicellular cyanobacteria with PSI dimer and tetramer near heterocyst-forming strains as one clade, HCR.

Additionally, the phylogenetic analysis provided a clear classification of PsaL correlating to the PSI oligomeric state (Supplementary Fig. 3). The major PSI oligomeric states can be predicted from the cyanobacterial *psaL* sequences, even though specific strains may deviate from the major correlation between PsaL and PSI oligomer; for example, the PSI monomer found in heterocyst-forming cyanobacteria (Supplementary Fig. 1). The formation of the tetrameric PSI may be a result of changes in the PsaL subunit, as previously proposed[22], and *psaL* genomic location in relation to *psaF–psaJ*, which may contribute to expression regulation and PSI assembly control. However, the differences in PsaL are not sufficient to cause PSI tetramer formation, consistent with the observations of PSI monomers in PCC 6803 expressing TS-821 PsaL. Besides differences in PsaL, other factors such as carotenoids and PSI assembly chaperones may contribute to the formation of tetrameric PSI.

The discovery of a pool of PSI interdimer carotenoids also suggests a possible physiological significance of tetrameric PSI over trimeric PSI, since these additional carotenoids may protect PSI from excessive influx of photons under HL. This inference is further supported by the fact that the carotenoid content, as well as the relative quantity and stability of PSI tetramer increased under HL (Figs. 5 and 6). Even under LL, PSI tetramer has a higher content of carotenoids compared with PSI trimer (Supplementary Fig. 9). This is in line with the observations of antennae cooperativity between the three *T. elongatus* PSI monomers that yield an increased optical cross-section of the trimer[35,36], whereas tetrameric and dimeric PSI did not show significant cooperativity among monomers[22]. In sum, tetrameric PSI alone, compared with trimeric PSI, is a less efficient form of PSI for light harvesting but a better form of PSI in relation to dissipation of excess photonic energy under HL conditions, thereby avoiding photoinhibition. Thus, these cyanobacteria can alter the oligomeric state of PSI under increasing light conditions while also increasing the content of photoprotective carotenoids. It is not clear whether it is the increase in the carotenoids that facilitates the formation of the tetramer or vice versa, but it is attractive to speculate that the tetrameric structure provides a mechanism to accumulate carotenoids, possibly via an unknown carotenoid-binding mechanism. The light-responsive adaptive behaviour of the PSI oligomeric

state and the ability of a PSI tetramer to adjust its carotenoid content represents an early evolutionary and unique photoprotective mechanism in HCR.

Exposure to HL may be the driving force for a change in PSI oligomerization. The shift of PSI oligomeric structure from trimeric to tetrameric under HL intensities supports that the HL condition associated with terrestrial environments may have been the selection pressure for PSI tetramer formation. *Synechocystis* sp. PCC 6803, although it has mainly trimeric PSI, accumulates more PSI monomer when grown under HL[37], suggesting that monomeric PSI may also be advantageous over trimeric PSI under increased light intensity. Our study on *Chroococcidiopsis* sp. PCC 7203, which has mostly monomeric PSI and some dimeric PSI, showed no obvious oligomeric shift when transferred from LL to HL (Supplementary Fig. 6). Whether monomeric PSI is a further adaptation to HL remains to be investigated.

Nevertheless, it is reasonable to speculate that early plastid ancestors of green algae and plants, and probably ancestors of HCR, needed to be able to cope with HL irradiance as they moved from relatively light-limiting aquatic settings to the surface of a terrestrial environment. These ancestral plastids and cyanobacteria would have benefited from having a PSI tetramer or monomer that is more adapted to HL intensity. These PSI oligomers are also well suited for the addition of other PSI subunits such as PsaH and light-harvesting complexes that bind to the inter-monomer faces of PSI. The observation of a very similar PSI tetramer in the glaucophyte *Cyanophora paradoxa*[3] suggests that the closest cyanobacterial relative to plastid ancestors may also have had tetrameric PSI, reinforcing the evidence of the gene homologies and phylogenomic conclusions that heterocyst-forming cyanobacteria are the most closely related to the plastid ancestor[38]. Yet, this view of plastid origin is contradictory to recent research pointing towards the deep branching cyanobacterium *Gloeomargarita lithophora* as the closest relative to the common plastid ancestor of glaucophytes, red algae, green algae and plants[39,40]. If this theory of deep branching cyanobacteria being the closest relative to ancestor of Archaeplastida holds, then the structural shift of PSI oligomer away from a trimer and the adaptation of photosynthesis to a HL environment in HCR, green algae and plants are examples of convergent evolution in photosynthesis.

Our results support the hypothesis that PSI oligomers evolved from trimeric to tetrameric in cyanobacteria en route to exclusively monomeric in plants and green algae. An earlier hypothesis, by comparing PSI trimeric structure from cyanobacteria and PSI monomeric structure from plants suggested that PSI evolved from a trimer to a monomer due to the presence of PsaH, which prevents the formation of the PSI trimer[41]. However, the presence of exclusively monomeric PSI in cyanobacteria (Supplementary Fig. 1), red algae and heterokonts[42] without the involvement of PsaH suggests that PSI monomerization preceded the introduction of the PsaH subunit. Changes in PsaL appear to be sufficient for PSI monomerization, notably with *Synechocystis* expressing *Arabidopsis* PsaL exhibiting exclusively monomeric PSI (Fig. 3b). Therefore, plant PsaL appears to be biochemically more closely related to cyanobacterial PsaL in relation to tetrameric and monomeric PSI. The presence of exclusively monomeric PSI in heterocyst-forming cyanobacteria (Supplementary Fig. 1) or mostly monomeric PSI in examples such as *Chroococcidiopsis* sp. PCC 7203 (Fig. 1a and Supplementary Fig. 1) suggests that the monomerization of PSI in plants and green algae shared the same or a closely related route to that of PSI tetramer formation during evolution.

Methods

Cyanobacterial growth conditions. The routine growth conditions for three control strains, *Synechocystis* sp. PCC 6803 (WT and mutants), *Chroococcidiopsis* sp. TS-821 (TS-821) and *T. elongatus* BP-1 were described in an earlier study[22]. Cyanobacteria from UTEX were maintained as recommended by the Culture Collection Center at University of Texas, Austin and the Pasteur Culture Collection of Cyanobacteria at the Institut Pasteur, Paris (standard culture conditions are presented in the Supplementary Data). To achieve sufficient cell mass for PSI oligomer identification, the cyanobacteria were cultured in feasible media with light intensity in the range of 20–100 µmol photons $m^{-2} s^{-1}$ (Supplementary Data). The modified ASNIII medium contains BG-11 medium with addition of ASNIII medium major salts (25 g l^{-1} NaCl, 3.5 g l^{-1} $MgSO_4 \cdot 7H_2O$, 2.0 g l^{-1} $MgCl_2 \cdot 6H_2O$ and 0.5 g l^{-1} KCl).

To study the physiological significance of PSI tetramer in cyanobacteria, non-standard culture conditions were tested. To investigate the effect of nitrogen sources, some heterocyst-forming cyanobacteria were cultured separately in BG-11, BG-110 or BG-11 + NH_4^+ (BG-11 supplemented with 1 mM NH_4Cl two days before collecting cells). To test the effect of temperature, some thermophilic cyanobacteria were cultured at 45 °C versus 37 °C. In addition, a culture of *Fischerella muscicola* PCC 7414 grown at 37 °C was incubated at 24 °C before collection. To investigate the effect of salinity, some marine cyanobacteria were cultured in both BG-11 and modified ASNIII media.

The standard HL and LL comparison experiments for TS-821, PCC 7414, PCC 7428 and PCC 7203 were done as described before[23]. To eliminate the potential stress from cell culture density and/or differences from lighting sources, a systematic analysis of how TS-821 respond to different levels of light intensity was done by culturing similar inoculum in a photobioreactor for two days under five light conditions (50, 100, 200, 400 and 800 µmol photons $m^{-2} s^{-1}$). For each light condition, half of the light intensity was provided by white LEDs and the other half was from red LEDs. The mid-log phase TS-821 cell (optical density at 680 nm (OD 680) 0.6–0.8) cultures under white light fluorescent light were inoculated in the 2 l bioreactor to a starting OD 680 of 0.04 (measured with a fluorometer probe from Photon Systems Instruments) before turning on the bioreactor lights. Cells were collected and stored −20 °C before PSI oligomer analysis.

Thylakoid membrane isolation. For thylakoid membrane preparation, cells were lysed by French press. Cyanobacterial cell pellets were washed in buffer A (50 mM MES-NaOH, pH 6.5, 5 mM $CaCl_2$ and 10 mM $MgCl_2$) and then pelleted by centrifugation[43]. Cell pellets were resuspended in lysis buffer (buffer A containing 0.5 M sorbitol) and homogenized by French press. In the case of *Scytonema crispum* UTEX LB 1556, cell aggregates were broken into small fragments by grinding in liquid nitrogen before resuspension in lysis buffer and homogenization. Homogenized cell suspensions were processed through the French press three times at 1,500 or 2,000 psi (10 to 14 MPa), then unbroken cells were removed by pelleting at 10,000*g* for 5 min.

In most cases, thylakoid membranes were pelleted from cell lysate by centrifugation at 40,000 r.p.m. (193,000*g* in a Type 50.2 Ti rotor, Beckman) for 30 min at 4 °C. Thylakoid membrane pellets were resuspended in buffer A + 12.5% glycerol and homogenized before storing at −20 °C or −80°C. For HL versus LL experiments, thylakoids were washed in buffer A once and pelleted at 193,000*g* for 15 min before final resuspension. In some special cases where cell mass was low and large membrane fragments could be pelleted at lower *g* forces, thylakoids were resuspended after spinning at 10,000*g* for 5 min. Chl concentration was determined as described previously[44].

PAGE analyses and western blot. In most cases, 4–16% BN-PAGE gels (Invitrogen) were used to analyse solubilized thylakoids or isolated photosystems, according to the user manual and references[45,46]. In addition, laboratory-prepared BN-PAGE gels were used to analyse larger amounts of sample. To analyse PSI oligomeric states, thylakoid membranes were solubilized in different concentrations of DDM (Glycon) at 25 °C for 1.5 h. Insoluble material was removed by centrifugation at 180,000*g* for 5 min or 98,000*g* for 10 min at 4 °C. Supernatants were taken for BN-PAGE analysis. Gel images were taken before fixation and staining to identify green bands for photosystems. After Coomassie staining, gel images were taken using a UVP transilluminator to visualize proteins with lower abundance and for quantification. To identify the photosystems after BN-PAGE, a second dimension Tris-Tricine SDS–PAGE was used as described previously[22].

Western blots were used to detect the presence of PsaL in *Synechocystis* mutants. Protein bands were transferred from polyacrylamide gels to a 0.45 µm PVDF membrane (Millipore) using a blotting cassette (idEA). Membranes were blocked with TBS-T + 3% NFM (non-fat milk powder) at room temperature for 1 h. Primary antisera were diluted from 1:5,000 in TBS-T + 3% NFM, depending on their efficiency before treating the blocked membranes overnight at 4 °C. Secondary antibody (goat anti-rabbit) conjugated to horseradish peroxidase (HRP) was diluted in TBS-T + 3% NFM to 1:50,000 before treating the washed membranes for 1 h at room temperature. The targeted proteins were detected using chemiluminscence HRP substrate (Millipore) and the signal was recorded using a ChemiDoc XDS system (Bio-Rad).

Antigen design and antibody production. PsaL sequences are not sufficiently well conserved for antigen design from a single consensus sequence. To produce one antigen that could be used to antisera against all PsaL of interest in this study, that is, *Chroococcidiopsis* sp. TS-821, *Arabidopsis*, *T. elongatus* BP-1 and *Synechocystis* sp. PCC 6803, a chimeric protein (CATSPsaL) containing fragments of the

different PsaLs was designed. The Kolaskar and Tongaonkar antigenicity method[47] via the Immune Epitope Database (http://tools.immuneepitope.org/bcell/) and ABCpred[48] (http://www.imtech.res.in/raghava/abcpred/index.html) were used to predict suitable epitopes. The antigen sequence was aligned against different PsaL fragments and the predicted antigens to ensure a high probability of obtaining an antibody for each PsaL (Supplementary Fig. 10). In addition to the N-terminal fragments, the loop insertion between second and third transmembrane helices of TS-821 PsaL was also used to achieve high antigenicity for TS-821.

A synthetic CATSPsaL coding sequence (Integrated DNA Technologies) was cloned into pTYB2 (NEB) plasmid. The expression plasmid DNA was then transformed into *E. coli* ER2566 for antigen expression. IMPACT Chitin Resin (NEB) was used as column matrix for antigen purification. Antibody was produced at Pocono Rabbit Farm using the 91 d protocol on 2 rabbits. For PsaL antibody production, purified antigen at 1 mg ml was used as inoculum.

PSI isolation and characterization. Sucrose density gradient centrifugation (SDGC) was used for PSI isolation as described previously[22]. SDGC was also used to study PSI oligomeric states, as a parallel or complementary technique to BN-PAGE profiling. Thylakoid membranes containing 0.4 mg ml^{-1} Chl were solubilized in 0.6–1% DDM. After removing insoluble fragments, the solubilized membranes containing 1 mg Chl were loaded on a 10–30% sucrose density gradient in buffer A containing 0.01% DDM. This method showed comparable results with BN-PAGE analysis. For larger capacity loading of solubilized membrane (containing 1–3 mg Chl) on a sucrose density gradient, centrifugation was performed twice with the first 20–24 h spin followed by dialysis and another 24 h spin (SW32Ti, 30,000 r.p.m.). Lower ionic strength, such as 0.4× buffer A was tried in sucrose density gradients for PCC 7414 PSI but showed no observable difference for PSI profiles. Inter-dimer carotenoids (Fig. 4e) were isolated after SDGC following treatment of PSI tetramer with 5% DDM for at least 1 h at room temperature. Isolated PSI samples were dialysed before analysis. For the proteomic comparison between PSI trimers and PSI tetramers, isolated PSI oligomers were further purified by BN-PAGE and gel slices were analysed.

Low temperature (77K) fluorescence spectra were acquired with excitation wavelength at 430 nm and the emission spectra at 600–800 nm were recorded. Each emission spectrum was averaged from ten technical repeats to enhance signal-to-noise ratio. Absorption spectra of isolated proteins and pigments were taken using a Cary 300 UV-Vis spectrometer (Agilent). The sample buffers were used as blanks. For PSI oligomer absorption spectra comparisons, A_{680} was adjusted close to 0.5 or 1. The PSI absorption differences were calculated after normalizing the data at A_{680}. Electron microscopy and single particle analyses were done as described in previous studies[21,22]. Pigment analyses were done using high-performance liquid chromatography by DHI (Hørsholm, Denmark).

***psaL* gene cloning and TS-821 genome sequencing.** Most cyanobacterial DNA extraction for *psaL* cloning was done as described[22]. TS-821 DNA for genome sequencing and some cyanobacterial DNA for *psaL* cloning were extracted using the NucleoBond DNA isolation kit (Macherey-Nagel Inc.). For *psaL* cloning of heterocyst-forming cyanobacteria with unknown genome data, different primer sets (Supplementary Tables 1 and 2) from *psaF* and *gmk* genes were used to amplify the *psaL* gene and its flanking region. The cyanobacteria of interests were classified using their known DNA sequences or genus names to facilitate picking primer pairs. PCR products were ligated into pJET vectors using CloneJET PCR cloning kit (Thermo Fisher). Plasmids containing cloned *psaL* were sequenced by Sanger sequencing at University of Tennessee Genomics Core.

TS-821 culture was purified as described[32] before DNA extraction for genome sequencing. The DNA was submitted to University of Tennessee Genomic Core for sequencing using Illumina MiSeq Kit v.2 with 2 × 250 bp read length. The resulted FASTQ files were analysed using SPAdes (v.3.7.1)[49]. The assembled contigs were submitted to PATRIC[50] for annotation, which uses the RAST[51] system.

Phylogenetic and *psaL* analyses. The species tree was generated by a concatenation of 29 conserved proteins selected from the phylogenetic markers previously validated for cyanobacteria using a maximum-likelihood method as described previously[52]. Protein sequences were aligned using MAFFT v.7.307[53]; ambiguous and saturated regions were removed with BMGE v.1.12 (with the gap rate parameter set to 0.5)[54]. The best-fitting model of amino acid substitution for this dataset was selected with ProtTest v.3.2[55]. A maximum-likelihood phylogenetic tree was generated with the alignment using PhyML 3.1.0.2[56] using the LG amino acid substitution model with gamma-distributed rate variation (six categories), estimation of the proportion of invariable sites and exploring tree topologies. One-hundred bootstrap replicates were performed. The phylogenetic trees were displayed and annotated using the interactive tree of life (iTOL) online tool[57].

Genomic context of *psaL*, *psaI*, *psaF* and *psaJ* genes and PsaL protein sequences were extracted from the MicroScope platform[58], public databases and data generated in a previous study[59] or this study Supplementary Data). The logo plot for the PsaL linker was generated using the WebLogo 3 website (http://weblogo.threeplusone.com)[60].

Construction of *Synechocystis psaL* mutants. Some of the *psaL* mutants were obtained in a previous study[22] with low expression efficiency. To improve the expression level of exogenous PsaL, codon-optimized synthetic *psaL* DNAs in pBSK vector were obtained from Integrated DNA Technologies. Similar methods were used for cloning and *Synechocystis* transformation as described[22]. The mutants were named as *Synechocystis* sp. PCC 6803 expressing synthetic *Chroococcidiopsis* sp. TS-821/*A. thaliana psaL* (SCHL/SAtL).

Reporting summary. Further information on research design is available in the Nature Research Reporting Summary linked to this article.

Data availability

The cloned cyanobacterial *psaL* sequences have been deposited in GenBank with the accession numbers KY575410, KY575411, KY575412, KY575413, KY575414, KY575415, KY575416, KY575417, KY575418, KY575419, KY575420, KY575421, KY575422, KY575423 and KY575424. The TS-821 whole-genome shotgun project has been deposited at DNA Data Bank of Japan/European Nucleotide Archive/GenBank under the accession MVDI00000000. The version described in this paper is version MVDI01000000.

Received: 31 May 2019; Accepted: 4 November 2019;
Published online: 9 December 2019

References

1. Raymond, J. & Blankenship, R. E. in *Advances in Photosynthesis and Respiration* Vol. 24 (Ed. Goldbeck, J. H.) 669–681 (Springer, 2007).
2. Gardian, Z. et al. Organisation of photosystem i and photosystem iI in red alga *Cyanidium caldarium*: encounter of cyanobacterial and higher plant concepts. *Biochim. Biophys. Acta* **1767**, 725–731 (2007).
3. Watanabe, M., Kubota, H., Wada, H., Narikawa, R. & Ikeuchi, M. Novel supercomplex organization of photosystem I in *Anabaena* and *Cyanophora paradoxa*. *Plant Cell Physiol.* **52**, 162–168 (2011).
4. Ben-Shem, A., Frolow, F. & Nelson, N. Crystal structure of plant photosystem I. *Nature* **426**, 630–635 (2003).
5. Kouril, R., van Oosterwijk, N., Yakushevska, A. E. & Boekema, E. J. Photosystem I: a search for green plant trimers. *Photochem. Photobiol. Sci.* **4**, 1091–1094 (2005).
6. Veith, T. & Buchel, C. The monomeric photosystem I-complex of the diatom *Phaeodactylum tricornutum* binds specific fucoxanthin chlorophyll proteins (FCPs) as light-harvesting complexes. *Biochim. Biophys. Acta* **1767**, 1428–1435 (2007).
7. Wood, W. H. J. et al. Dynamic thylakoid stacking regulates the balance between linear and cyclic photosynthetic electron transfer. *Nat. Plants* **4**, 116–12 (2018).
8. Boekema, E. J. et al. Evidence for a trimeric organization of the photosystem I complex from the thermophilic cyanobacterium *Synechococcus* sp. *FEBS Lett.* **217**, 283–286 (1987).
9. Shubin, V. V., Bezsmertnaya, I. N. & Karapetyan, N. V. Isolation from *Spirulina* membranes of 2 photosystem i-type complexes, one of which contains chlorophyll responsible for the 77-K fluorescence band at 760 Nm. *FEBS Lett.* **309**, 340–342 (1992).
10. Shubin, V. V., Tsuprun, V. L., Bezsmertnaya, I. N. & Karapetyan, N. V. Trimeric forms of the photosystem I reaction center complex pre-exist in the membranes of the cyanobacterium *Spirulina platensis*. *FEBS Lett.* **334**, 79–82 (1993).
11. Tsiotis, G., Haase, W., Engel, A. & Michel, H. Isolation and structural characterization of trimeric cyanobacterial photosystem I complex with the help of recombinant antibody fragments. *Eur. J. Biochem.* **231**, 823–830 (1995).
12. Garczarek, L., van der Staay, G. W. M., Thomas, J. C. & Partensky, F. Isolation and characterization of photosystem I from two strains of the marine oxychlorobacterium *Prochlorococcus*. *Photosynth. Res.* **56**, 131–141 (1998).
13. Bibby, T. S., Mary, I., Nield, J., Partensky, F. & Barber, J. Low-light-adapted *Prochlorococcus* species possess specific antennae for each photosystem. *Nature* **424**, 1051–1054 (2003).
14. Boekema, E. J. et al. A giant chlorophyll–protein complex induced by iron defciency in cyanobacteria. *Nature* **412**, 745–748 (2001).
15. Tucker, D. L. & Sherman, L. A. Analysis of chlorophyll–protein complexes from the cyanobacterium *Cyanothece* sp. ATCC 51142 by non-denaturing gel electrophoresis. *Biochim. et Biophys.* **1468**, 150–160 (2000).
16. Casella, S. et al. Dissecting the native architecture and dynamics of cyanobacterial photosynthetic machinery. *Mol. Plant* **10**, 1434–1448 (2017).
17. MacGregor-Chatwin, C. et al. Lateral segregation of photosystem I in cyanobacterial thylakoids. *Plant Cell* **29**, 1119–1136 (2017).
18. Mangels, D. et al. Photosystem I from the unusual cyanobacterium *Gloeobacter violaceus*. *Photosynth. Res.* **72**, 307–319 (2002).
19. Almog, O., Shoham, G., Michaeli, D. & Nechushtai, R. Monomeric and trimeric forms of photosystem I reaction center of *Mastigocladus laminosus*: crystallization and preliminary characterization. *Proc. Natl Acad. Sci. USA* **88**, 5312–5316 (1991).

20. Jordan, P. et al. Three-dimensional structure of cyanobacterial photosystem I at 2.5 A resolution. *Nature* **411**, 909–917 (2001).
21. Watanabe, M. et al. Attachment of phycobilisomes in an antenna–photosystem I supercomplex of cyanobacteria. *Proc. Natl Acad. Sci. USA* **111**, 2512–2517 (2014).
22. Li, M., Semchonok, D. A., Boekema, E. J. & Bruce, B. D. Characterization and evolution of tetrameric photosystem I from the thermophilic cyanobacterium *Chroococcidiopsis* sp. TS-821. *Plant Cell* **26**, 1230–1245 (2014).
23. Semchonok, D. A., Li, M., Bruce, B. D., Oostergetel, G. T. & Boekema, E. J. Cryo-EM structure of a tetrameric cyanobacterial photosystem I complex reveals novel subunit interactions. *Biochim. Biophys. Acta* **1857**, 1619–1626 (2016).
24. Malavath, T., Caspy, I., Netzer-El, S. Y., Klaiman, D. & Nelson, N. Structure and function of wild-type and subunit-depleted photosystem I in Synechocystis. *Biochim. Biophys. Acta* **1859**, 645–654 (2018).
25. Gan, F. et al. Extensive remodeling of a cyanobacterial photosynthetic apparatus in far-red light. *Science* **345**, 1312–1317 (2014).
26. Gan, F. & Bryant, D. A. Adaptive and acclimative responses of cyanobacteria to far-red light. *Environ. Microbiol.* **17**, 3450–3465 (2015).
27. Qin, X., Suga, M., Kuang, T. & Shen, J. R. Structural basis for energy transfer pathways in the plant PSI–LHCI supercomplex. *Science* **348**, 989–995 (2015).
28. Mazor, Y., Borovikova, A. & Nelson, N. The structure of plant photosystem I super-complex at 2.8 A resolution. *eLife* **4**, e07433 (2015).
29. Cardona, T. et al. Electron transfer protein complexes in the thylakoid membranes of heterocysts from the cyanobacterium *Nostoc punctiforme*. *Biochim. Biophys. Acta* **1787**, 252–263 (2009).
30. Vintila, S. & El-Shehawy, R. Ammonium ions inhibit nitrogen fixation but do not affect heterocyst frequency in the bloom-forming cyanobacterium *Nodularia spumigena* strain AV1. *Microbiology* **153**, 3704–3712 (2007).
31. Vintila, S. & El-Shehawy, R. Variability in the response of the cyanobacterium *Nodularia spumigena* to nitrogen supplementation. *J. Environ. Monit.* **12**, 1885–1890 (2010).
32. Rippka, R., Deruelles, J., Waterbury, J. B., Herdman, M. & Stanier, R. Y. Generic assignments, strain histories and properties of pure cultures of cyanobacteria. *J. Gen. Microbiol.* **111**, 1–61 (1979).
33. Fewer, D., Friedl, T. & Budel, B. *Chroococcidiopsis* and heterocyst-differentiating cyanobacteria are each other's closest living relatives. *Mol. Phylogenet. Evol.* **23**, 82–90 (2002).
34. Shih, P. M. et al. Improving the coverage of the cyanobacterial phylum using diversity-driven genome sequencing. *Proc. Natl Acad. Sci. USA* **110**, 1053–1058 (2013).
35. Iwuchukwu, I. J. et al. Self-organized photosynthetic nanoparticle for cell-free hydrogen production. *Nat. Nanotechnol.* **5**, 73–79 (2010).
36. Baker, D. R. et al. Comparative photoactivity and stability of isolated cyanobacterial monomeric and trimeric photosystem I. *J. Phys. Chem. B* **118**, 2703–2711 (2014).
37. Wang, Q. et al. The high light-inducible polypeptides stabilize trimeric photosystem I complex under high light conditions in *Synechocystis* PCC 6803. *Plant Physiol.* **147**, 1239–1250 (2008).
38. Dagan, T. et al. Genomes of Stigonematalean cyanobacteria (subsection V) and the evolution of oxygenic photosynthesis from prokaryotes to plastids. *Genome Biol. Evol.* **5**, 31–44 (2013).
39. Sánchez-Baracaldo, P., Raven, J. A., Pisani, D. & Knoll, A. H. Early photosynthetic eukaryotes inhabited low-salinity habitats. *Proc. Natl Acad. Sci. USA* **114**, E7737–E7745 (2017).
40. Ponce-Toledo, R. I. et al. An early-branching freshwater cyanobacterium at the origin of plastids. *Curr. Biol.* **27**, 386–391 (2017).
41. Amunts, A. & Nelson, N. Plant photosystem I design in the light of evolution. *Structure* **17**, 637–650 (2009).
42. Alboresi, A. et al. Conservation of core complex subunits shaped the structure and function of photosystem I in the secondary endosymbiont alga *Nannochloropsis gaditana*. *New Phytol.* **213**, 714–726 (2017).
43. Watanabe, M., Iwai, M., Narikawa, R. & Ikeuchi, M. Is the photosystem II complex a monomer or a dimer? *Plant Cell Physiol.* **50**, 1674–1680 (2009).
44. Iwamura, T., Nagai, H. & Ichimura, S.-E. Improved methods for determining contents of chlorophyll, protein, bibonucleic acid, and deoxyribonucleic acid in planktonic populations. *Int. Rev. ges. Hydrobiol. Hydrogr.* **55**, 131–147 (1970).
45. Schägger, H. & von Jagow, G. Blue native electrophoresis for isolation of membrane protein complexes in enzymatically active form. *Anal. Biochem.* **199**, 223–231 (1991).
46. Wittig, I., Braun, H.-P. & Schagger, H. Blue native PAGE. *Nat. Protoc.* **1**, 418–428 (2006).
47. Kolaskar, A. S. & Tongaonkar, P. C. A semi-empirical method for prediction of antigenic determinants on protein antigens. *FEBS Lett.* **276**, 172–174 (1990).
48. Saha, S. & Raghava, G. P. S. Prediction of continuous B-cell epitopes in an antigen using recurrent neural network. *Proteins* **65**, 40–48 (2006).
49. Bankevich, A. et al. SPAdes: a new genome assembly algorithm and its applications to single-cell sequencing. *J. Comput. Biol.* **19**, 455–477 (2012).
50. Wattam, A. R. et al. PATRIC, the bacterial bioinformatics database and analysis resource. *Nucleic Acids Res.* **42**, D581–D591 (2014).
51. Overbeek, R. et al. The SEED and the Rapid Annotation of microbial genomes using Subsystems Technology (RAST). *Nucleic Acids Res.* **42**, D206–D214 (2014).
52. Calteau, A. et al. Phylum-wide comparative genomics unravel the diversity of secondary metabolism in cyanobacteria. *BMC Genomics* **15**, 977 (2014).
53. Katoh, K. & Standley, D. M. MAFFT multiple sequence alignment software version 7: Improvements in performance and usability. *Mol. Biol. Evol.* **30**, 772–780 (2013).
54. Criscuolo, A. & Gribaldo, S. BMGE (Block Mapping and Gathering with Entropy): a new software for selection of phylogenetic informative regions from multiple sequence alignments. *BMC Evol. Biol.* **10**, 210 (2010).
55. Darriba, D., Taboada, G. L., Doallo, R. & Posada, D. ProtTest 3: Fast selection of best-fit models of protein evolution. *Bioinformatics* **27**, 1164–1165 (2011).
56. Guindon, S. et al. New algorithms and methods to estimate maximum-likelihood phylogenies: Assessing the performance of PhyML 3.0. *Syst. Biol.* **59**, 307–321 (2010).
57. Letunic, I. & Bork, P. Interactive tree of life (iTOL) v3: An online tool for the display and annotation of phylogenetic and other trees. *Nucleic Acids Res.* **44**, W242–W245 (2016).
58. Vallenet, D. et al. MicroScope in 2017: An expanding and evolving integrated resource for community expertise of microbial genomes. *Nucleic Acids Res.* **45**, D517–D528 (2017).
59. Schirrmeister, B. E., Gugger, M. & Donoghue, P. C. Cyanobacteria and the Great Oxidation Event: evidence from genes and fossils. *Palaeontology* **58**, 769–785 (2015).
60. Crooks, G. E., Hon, G., Chandonia, J. M. & Brenner, S. E. WebLogo: A sequence logo generator. *Genome Res.* **14**, 1188–1190 (2004).

Acknowledgements

Support to B.D.B., M.L. and J.T.N. was provided by the Gibson Family Foundation, the Bredesen Center for Interdisciplinary Research and Education, the Tennessee Plant Research Center, a UTK Professional Development Award, the Dr. Donald L. Akers Faculty Enrichment Fellowship to B.D.B. and National Science Foundation support to B.D.B. (DGE-0801470 and EPS-1004083). M.L. has been supported as a CIRE Fellow at University of Tennessee, Knoxville. A Professional Development Award from the Graduate School at UTK supported travel of B.D.B. to the Netherlands and to the Institut Pasteur. NWO Chemical Sciences supported work at University of Groningen. J.P.W. has been supported by NIH P30 DK063491. The Institut Pasteur supported Pasteur Culture Collection of cyanobacteria. We thank Y. I. Park for the use of the cyanobacterial genome of PCC 7124, and N.G. Brady and T. Cardona for helpful comments on the manuscript.

Author contributions

M.L., M.G. and B.D.B. designed the research. M.L. carried out most of the biochemistry and molecular biology experiments. A.C. performed phylogenetic and bioinformatics analyses. D.A.S. and E.J.B. did the electron microscopy imaging and single-particle analyses. T.A.W. did most of the *psaL* cloning. N.S. and J.T.N. prepared most of the cell materials. J.T.N. carried out the spectral comparison of PCC 7414 PSI oligomers J.W. performed the proteomic analyses. M.L. and B.D.B. wrote the article and all other authors contributed in editing and revising the article.

Competing interests

The authors declare no competing interests.

Additional information

Supplementary information is available for this paper at https://doi.org/10.1038/s41477-019-0566-x.

Correspondence and requests for materials should be addressed to B.D.B.

Peer review information Nature Plants thanks Conrad Mullineaux, Ann Magnuson and the other, anonymous, reviewer for their contribution to the peer review of this work.

Reprints and permissions information is available at www.nature.com/reprints.

Publisher's note Springer Nature remains neutral with regard to jurisdictional claims in published maps and institutional affiliations.

nature research

Corresponding author(s): Barry D Bruce

Last updated by author(s): Oct 8, 2019

Reporting Summary

Nature Research wishes to improve the reproducibility of the work that we publish. This form provides structure for consistency and transparency in reporting. For further information on Nature Research policies, see Authors & Referees and the Editorial Policy Checklist.

Statistics

For all statistical analyses, confirm that the following items are present in the figure legend, table legend, main text, or Methods section.

n/a	Confirmed
☐	☒ The exact sample size (*n*) for each experimental group/condition, given as a discrete number and unit of measurement
☐	☒ A statement on whether measurements were taken from distinct samples or whether the same sample was measured repeatedly
☒	☐ The statistical test(s) used AND whether they are one- or two-sided *Only common tests should be described solely by name; describe more complex techniques in the Methods section.*
☒	☐ A description of all covariates tested
☒	☐ A description of any assumptions or corrections, such as tests of normality and adjustment for multiple comparisons
☒	☐ A full description of the statistical parameters including central tendency (e.g. means) or other basic estimates (e.g. regression coefficient) AND variation (e.g. standard deviation) or associated estimates of uncertainty (e.g. confidence intervals)
☒	☐ For null hypothesis testing, the test statistic (e.g. *F*, *t*, *r*) with confidence intervals, effect sizes, degrees of freedom and *P* value noted *Give P values as exact values whenever suitable.*
☒	☐ For Bayesian analysis, information on the choice of priors and Markov chain Monte Carlo settings
☐	☐ For hierarchical and complex designs, identification of the appropriate level for tests and full reporting of outcomes
☒	☐ Estimates of effect sizes (e.g. Cohen's *d*, Pearson's *r*), indicating how they were calculated

Our web collection on statistics for biologists contains articles on many of the points above.

Software and code

Policy information about availability of computer code

Data collection	No special software was used for data collection except those installed for instruments, see Methods for instruments used.
Data analysis	The following softwares or web-services are used for data analyses: ABCpred, IEDB Analysis Resource, SPAdes (version 3.7.1), RAST system, MAFFT v7.307, BMGE v1.12, ProtTest v3.2, PhyML 3.1.0.2, interactive tree of life (iTOL), WebLogo, GraphPad Prism Ver. 8. Detailed references or links to resources are provided in the Methods section.

For manuscripts utilizing custom algorithms or software that are central to the research but not yet described in published literature, software must be made available to editors/reviewers. We strongly encourage code deposition in a community repository (e.g. GitHub). See the Nature Research guidelines for submitting code & software for further information.

Data

Policy information about availability of data

All manuscripts must include a data availability statement. This statement should provide the following information, where applicable:

- Accession codes, unique identifiers, or web links for publicly available datasets
- A list of figures that have associated raw data
- A description of any restrictions on data availability

The cloned cyanobacterial psaL sequences can be found in GenBank through the following acces-sion numbers: KY575410, KY575411, KY575412, KY575413, KY575414, KY575415, KY575416, KY575417, KY575418, KY575419, KY575420, KY575421, KY575422, KY575423, KY575424. TS-821 Whole Genome Shotgun project has been deposited at DDBJ/ENA/GenBank under the accession MVDI00000000. The version described in this paper is version MVDI01000000.

Field-specific reporting

Please select the one below that is the best fit for your research. If you are not sure, read the appropriate sections before making your selection.

☒ Life sciences ☐ Behavioural & social sciences ☐ Ecological, evolutionary & environmental sciences

For a reference copy of the document with all sections, see nature.com/documents/nr-reporting-summary-flat.pdf

Life sciences study design

All studies must disclose on these points even when the disclosure is negative.

Sample size	n = 5 was used to calculate trimeric PSI fraction in native gel (Figure 5). Other experiments with technical/biological repeats were described in each figure legend where applicable.
Data exclusions	The 0.4% DDM lane for 800 umol/m2/s condition has little trimeric PSI, so the 0.4% DDM solubilization condition was excluded for comparison.
Replication	Most experiments have technical/biological repeats to confirm the experimental findings. Some experiments were done once with different materials/methods to confirm similar findings/conclusions.
Randomization	Not relevant
Blinding	Not relevant

Reporting for specific materials, systems and methods

We require information from authors about some types of materials, experimental systems and methods used in many studies. Here, indicate whether each material, system or method listed is relevant to your study. If you are not sure if a list item applies to your research, read the appropriate section before selecting a response.

Materials & experimental systems

n/a	Involved in the study
☐	☒ Antibodies
☒	☐ Eukaryotic cell lines
☒	☐ Palaeontology
☒	☐ Animals and other organisms
☒	☐ Human research participants
☒	☐ Clinical data

Methods

n/a	Involved in the study
☒	☐ ChIP-seq
☒	☐ Flow cytometry
☒	☐ MRI-based neuroimaging

Antibodies

Antibodies used	non-commercial, Anti-PsaL Rabbit Serum described in Methods
Validation	Pocono Rabbits Farm generated the anti-PsaL serum using purified antigen; validated by data provided in the manuscript.